SCIENTIFIC REPORTS

OPEN

SUBJECT AREAS:
CARBON NANOTUBES AND FULLERENES
NANOSCIENCE AND TECHNOLOGY
NANOSCALE MATERIALS

Received
27 September 2013

Accepted
10 December 2013

Published
8 January 2014

Correspondence and requests for materials should be addressed to J.Z. (jzhong@suda.edu.cn) or X.H.S. (xhsun@suda.edu.cn)

Revealing the Role of Catalysts in Carbon Nanotubes and Nanofibers by Scanning Transmission X-ray Microscopy

Jing Gao, Jun Zhong, Lili Bai, Jinyin Liu, Guanqi Zhao & Xuhui Sun

Soochow University-Western University Centre for Synchrotron Radiation Research, Institute of Functional Nano and Soft Materials Laboratory (FUNSOM) and Collaborative Innovation Center of Suzhou Nano Science & Technology, Soochow University, Suzhou 215123, China.

The identification of effective components on the atomic scale in carbon nanomaterials which improve the performance in various applications remains outstanding challenges. Here the catalyst residues in individual carbon nanotube (CNT) and carbon nanofiber (CNF) were clearly imaged with a concurrent characterization of their electronic structure by nanoscale scanning transmission X-ray microscopy. Except for prominent catalyst nanoparticle at the tip, tiny catalyst clusters along the tube (fiber) were detected, indicating a migration of the catalysts with the growth of CNTs (CNFs). The observation provides the direct evidence on the atomic metal in CNT for oxygen reduction reported in the literature. Interaction between catalysts (Fe, Ni) and CNTs (CNFs) at the tip was also identified by comparing the X-ray absorption spectra. A deep understanding of catalyst residues such as Fe or Ni in carbon nanomaterials is very vital to growth mechanism development and practical applications.

Carbon-based materials containing metals (such as Fe or Co) and nitrogen impurities have been considered to be good alternatives to precious-metal electrocatalysts for the oxygen reduction reaction (ORR) in fuel cells[1–6]. Nitrogen doping in carbon nanotubes (CNTs) or graphene has been studied and shown to be a key role for the high ORR activity[3–5]. However, because of the complex compositions in carbon materials such as the existence of amorphous carbon, catalyst residues, various structural defects and surface contaminations, the identification of effective components in carbon-based materials which improve the performance and the understanding of the nature of ORR catalytic sites on the atomic scale still remain outstanding challenges[6,7]. For example, the extremely small amounts of irons originated from nanotube growth seeds were recently revealed to play very important role in facilitating the formation of catalytic sites and boosting the activity of the catalyst together with nitrogen species[6]. The iron and nitrogen atoms in the few-walled CNTs attached with nanoscale graphene sheets were clearly imaged by annular dark-field (ADF) and atomic-scale electron energy loss spectrum (EELS) imaging in aberration-corrected scanning transmission electron microscopy (STEM)[6]. It is thus important to explore the form of catalyst residues such as Fe or Ni in carbon nanomaterials with the identification of their electronic structure, which may help for the understanding of the growth mechanism of carbon nanomaterials and their functionality in practical applications.

Scanning transmission X-ray microscopy (STXM) has been considered to be an effective tool to localize and characterize the electronic structure of carbon nanomaterials[8–14]. STXM combines both X-ray absorption near-edge structure (XANES) spectroscopy and microscopy with a spatial resolution of a few tens of nanometers[12]. XANES is an element-specific spectroscopic technique involving the excitation of electrons from a core level to local and partial empty states of a defined character[12,14]. The combination of classical XANES method with a high spatial resolution in STXM provides a unique capability to explore electronic and structural information in carbon nanomaterials[8–14]. Here by employing STXM, Fe and Ni residues, the widely used catalyst in the CNT/CNF growth[15,16], in individual CNT and CNF were imaged with a concurrent identification of their electronic structure. Interestingly, we found that the catalyst may migrate with the growth of CNT (CNF) through the whole CNT (CNF) as tiny clusters or even atomic metal, which provides the direct evidence on the existence of the atomic metal for the ORR[6]. Moreover, the catalyst nanoparticles at the tip of CNT (CNF) show a strong interaction with carbon as metal-carbon bonds, as revealed by the XANES spectra.

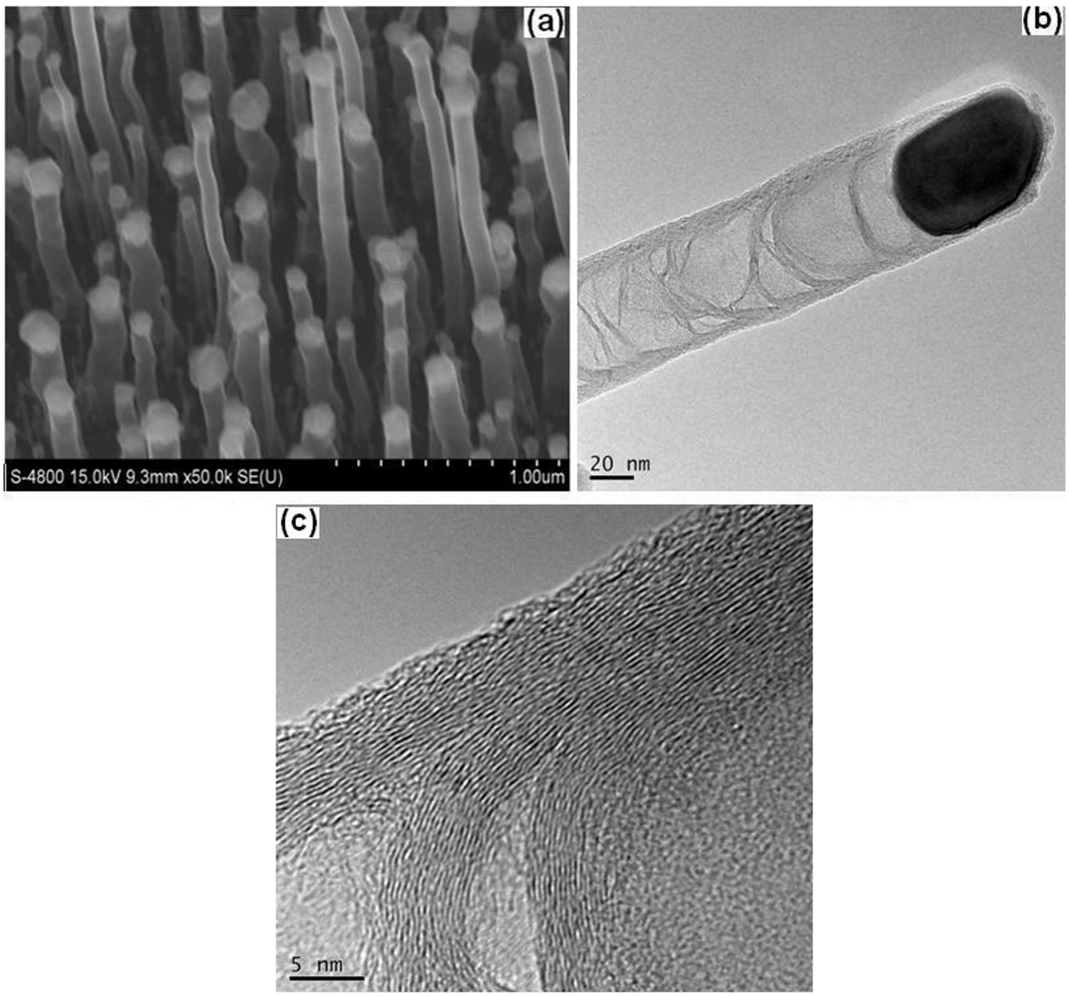

Figure 1 | (a) SEM and (b) TEM images of CNTs grown with 20 nm Fe/Ti underlayer. (c) Magnified TEM image of CNTs.

Results

Fig. 1 shows the scanning electron microscopy (SEM) and transmission electron microscopy (TEM) images of CNTs synthesized with Fe catalysts (20 nm Fe/Ti underlayer). SEM image (Fig. 1a) reveals the aligned structure of CNTs on substrate. TEM image (Fig. 1b) shows a tube-like structure with a hollow center and thin tube wall. A Fe catalyst about 100 nm at the tip of CNT can be observed.

Fig. 2 shows the STXM results and TEM image. The TEM image (Fig. 2a) shows the presence of CNTs. An individual CNT with Fe catalyst nanoparticle (diameter about 100 nm) at the tip can be observed. To compare the different electronic structures in CNT (with and without Fe catalyst), 4 different parts were marked with rectangles and numbers (denoted as tube1–4). The part between tube2 and tube3 is an overlap of CNT and TEM grid with lacey carbon thus we have not shown the XANES spectrum. Fig. 2b shows the STXM map of the same region at C *K*-edge. The STXM map is in good agreement with the TEM image.

The XANES spectra of different parts of the tube (tube1–4) at C *K*-edge are shown in Fig. 2c. Typically, the XANES spectra for tube1–4 show three main absorption features: A, B and D at about 285.5, 288.5 and 291.7 eV, respectively. The corresponding assignment of the absorption features has been well studied[14,17]. Feature A originates from the π^* excitation in a carbon ring structure, feature D from the σ^* excitation, while feature B from the transitions to sp^3 hybridized states due to oxygenated groups and/or surface contaminations[14,17]. The spectra have been normalized at the σ^* excitation to reveal the difference between 282 and 292 eV. All four parts show clear features A and D while a weak feature B can be observed, indicating weak oxidation or other surface modification. The spectral resolution for tube1 with Fe catalyst is worse compared to that for other parts, which can be attributed to less carbon content at the tip. However, a strong peak at about 283.5 eV (marked as A1) can be obviously observed for tube1. The peak position is about 2 eV lower than the π^* excitation. Liu *et al.* reported a similar peak at lower energy than the π^* excitation in $FeCl_3$ intercalated CNTs and assigned it to the new empty states induced by a charge transfer process between carbon and $FeCl_3$[18]. Here with a good spatial resolution the STXM results with a prominent XANES peak at 283.5 eV clearly reveal that at the connection part (tube1) there is a strong Fe-C interaction (chemical bonds) between Fe catalyst and CNT, which may help to understand the growth mechanism of CNTs. Metal nanoparticles play an important role as catalyst for CNT growth which may help to produce CNTs with desired atomic structures selectively for electronic technology and industry. However, there have been a number of controversial hypotheses, theoretical simulations, and experiments on the growth process of CNTs[19–21]. For example, the tube grows along the interface between nanoparticle and carbon and one of the crucial questions on the growth mechanism of CNTs is whether the nanoparticles are carbide particles with a strong interface interaction between carbon and metal catalyst (Metal-Carbon interaction) or pure metal particles[21]. TEM results showed the existence of Fe_3C by the electron diffraction pattern but they were not spectroscopic evidence revealing the electronic structure and bonds[19–21]. In-situ X-ray photoelectron spectroscopy (XPS)

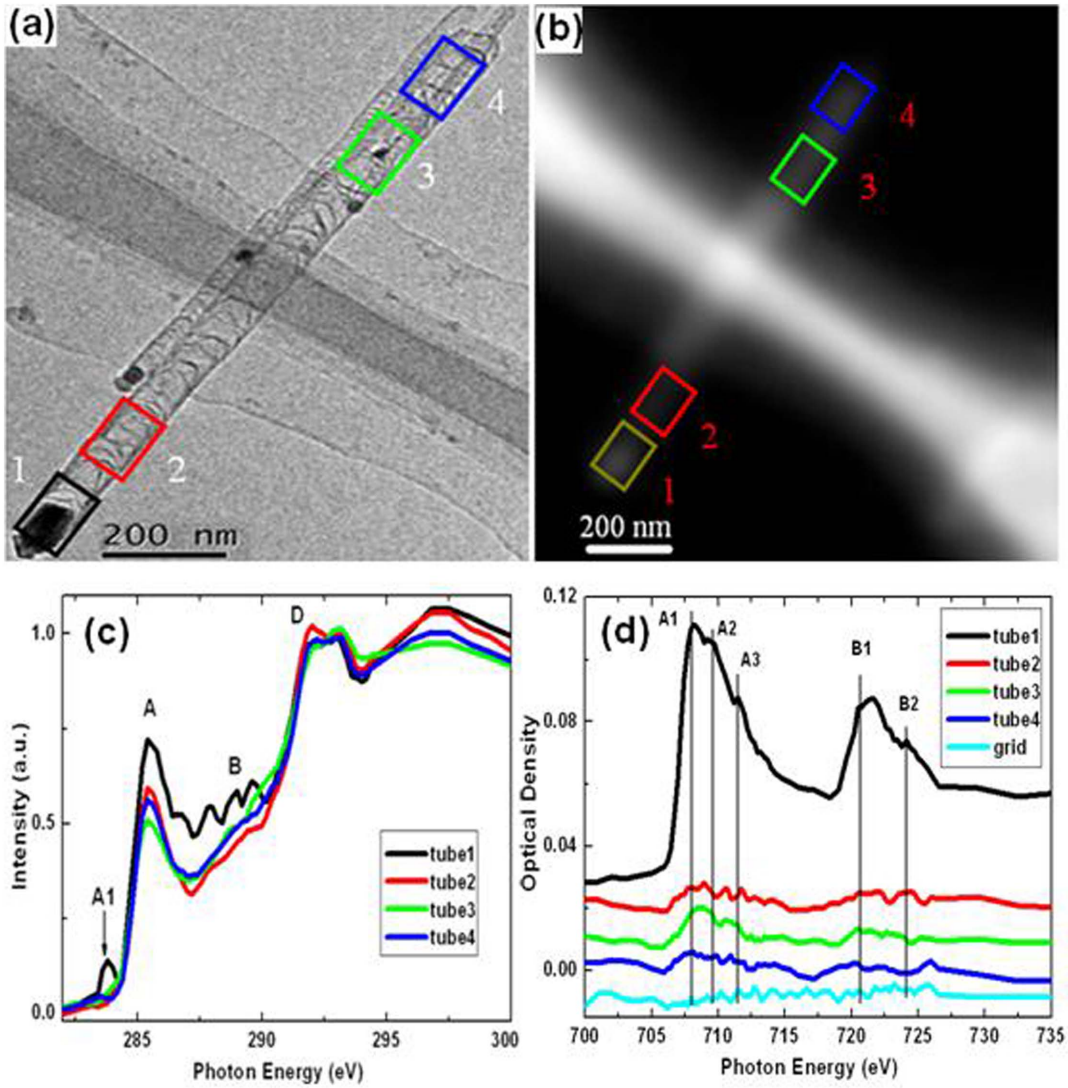

Figure 2 | **(a) TEM image and (b) STXM map (at C *K*-edge) of CNTs, (c) Normalized C *K*-edge XANES spectra of tube1–4 labeled in Fig. 2a and b, (d) Fe *L*-edge XANES spectra of tube1–4 labeled in Fig. 2a and b.**

was also used to probe the Fe-C bonds for CNTs synthesized by CVD method[19]. A peak at about 283.2 eV in the XPS spectra indicated the Fe-C interaction. However, the XPS signal represented a spatial average over the accessible catalyst particle surface in the beam area and the contribution from contaminations or other carbon source such as amorphous carbon could not be excluded. Here our XANES spectra with a good spatial resolution clearly identify the Fe-C interaction indicating the existence of carbide particles.

Fig. 2d shows the Fe *L*-edge XANES spectra of tube1–4. The spectra were normalized to the incident flux and the peak intensity is proportional to content of Fe element. It is clear that tube1 shows prominent features for the presence of Fe catalyst at the tip, which is in good agreement with the TEM image. The spectrum of tube1 shows two main features at about 707 eV (A1–A3) and 721 eV (B1–B2) for Fe L_3 and L_2 edge resonances, respectively. A strong peak at about 707 eV (labeled with A1) and two relative weak features at about 709 eV and 712 eV (labeled with A2 and A3) can be observed for tube1. According to the literature[22], the strong peak A1 indicates that the Fe catalyst in CNT has a low chemical state such as Fe metal or Fe^{2+}. A more oxidative state such as iron oxide will show prominent features A2 and A3, while a decrease of feature A1 can be observed[22]. For tube3, there is a small tube attached on the big tube and a small Fe catalyst at the tip can also be observed from the TEM image. Thus the XANES spectrum for tube3 also shows Fe L_3 and L_2 edge resonances. However, weak XANES features for Fe can be also observed for tube2 and tube4, while no obvious Fe nanoparticle can be observed in these parts from the TEM image. The XANES features are weak but clear, which strongly suggest the existence of Fe in tube2 and tube4. For comparison, the spectrum of TEM grid with lacey carbon (background) is also shown but no signal of Fe can be observed.

Recently the extremely small amounts of irons originated from nanotube growth seeds were reported to be very important for the high ORR activity. The atomic iron in the outside graphene sheets of few-walled CNTs were imaged by STEM[6]. Here our results confirm the existence of tiny Fe throughout the CNTs. In the synthesis process, the catalysts fluctuate structurally as liquid-like phase as reported in the literature[19,21]. The catalysts may migrate with the growth of CNTs and leave in the layers of CNTs as the clusters (or atomic metal). The clusters (or atomic metal) are too small to be observed compared to the big one at the tip. Here by STXM the XANES features clearly reveal the existence of tiny Fe clusters (or atomic metal) on the surface of CNTs. The results may help to explain the origin of atomic metal in CNTs observed in the literature which showed important role for the improved ORR activity[21]. The small amounts of irons responsible for ORR activity may not only

originate from the catalyst seeds[21], but also from the migrated metal with the growth of CNTs.

The electronic structure of Fe in CNTs is also measured by XANES and the results suggest it is a low chemical state similar to Fe metal or Fe^{2+}, as shown in Fig. 2d. It should be useful to know that the Fe in CNTs with a low chemical state. In Fig. 1c the high-resolution TEM image of the same tube (from tube2) is also shown. It is difficult to observe the clusters in CNT suggesting that the existence form of Fe is tiny clusters with the size smaller than 1 nm or is even at atomic scale (with possible Fe-C interaction).

The electronic structure of CNFs synthesized with Ni catalysts was also explored by STXM. Fig. 3 shows the SEM and TEM images of CNFs synthesized with Ni catalysts (20 nm Ni/Ti underlayer). SEM image (Fig. 3a) reveals the aligned structure of CNFs on substrate. Compared to the TEM image in Fig. 1b with a tube-like structure of CNTs with Fe catalysts, the TEM image in Fig. 3b shows a small hollow center and a thick wall. The thick wall shows the stacking cone-like structure without clear concentric cylindrical carbon layers as that for multi-walled carbon nanotubes (MWCNTs). The ratios of the wall to the inner hollow structure are very big and in some literatures the structure was also attributed to carbon nanofiber (CNF)[16]. Ni catalysts can be observed at the tip of different CNFs in Fig. 3b. The CNFs at the center of the circle in Fig. 3b is to be measured by STXM.

Fig. 4 shows the STXM results and HR-TEM image of CNF. An individual CNF with Ni catalyst nanoparticle at the tip can be observed in Fig. 4a. For comparison, 4 different parts were marked with rectangles and numbers (denoted as fiber1–4). Fig. 4b shows the STXM map at C *K*-edge, which is in good agreement with the TEM image. The XANES spectra of fiber1–4 at C *K*-edge have been shown in Fig. 4c. Fig. 4d shows the Ni *L*-edge XANES spectra of fiber1–4. We also replotted the Ni *L*-edge XANES spectra with normalized intensity in Fig. 5.

Discussion

In Fig. 4c, similar to the results for CNT, a strong peak at about 283.5 eV can be observed for fiber1 suggesting the interaction between Ni and CNF[23]. The results for both Fe and Ni catalysts strongly confirm the existence of the interaction between the catalysts and CNTs (or CNFs) in the growth process.

In Fig. 4d it is clear that fiber1 shows clear features for the presence of Ni catalyst. The spectrum of fiber1 shows two main features around 853 eV (A1–A2) and 870 eV (B1–B2) for Ni L_3 and L_2 edge resonances, respectively. For Ni L_3 edge, a strong peak at about 852.5 eV (labeled with A1) can be observed with a relative weak shoulder at about 854.5 eV (labeled with A2). According to the literature[24], the strong peak A1 stands for a low chemical state such as Ni metal, while a more oxidative state such as NiO will show a prominent feature A2. The strong XANES feature A1 and relatively weak A2 for fiber1 suggest that the Ni catalyst at the tip is mainly Ni metal[24]. Fiber2 also shows clear features for Ni since this part also cover some Ni catalyst as observed from the TEM image. However, for the parts without obvious Ni catalysts (fiber3 and fiber4), weak but clear XANES features for Ni can also be observed, which is similar to the results for CNT with Fe catalysts. The XANES features clearly reveal the existence of Ni on the fiber, which could also be tiny Ni clusters smaller than 1 nm or even at atomic scale as that for Fe in CNTs.

In Fig. 5 we show the normalized Ni *L*-edge XANES spectra of fiber1–4. The signals for fiber3 and fiber4 are weak and the spectra are not as smooth as that for fiber1 and fiber2. However, the spectra for fiber3 and fiber4 show clear XANES features which are different from those for fiber1 and fiber2. Compared to Ni metal in fiber1 and fiber2 which shows a strong A1 and weak A2, the spectra for fiber3 and fiber4 show a relative weak A1 but a strong feature A2 which suggest that a more oxidative state such as NiO in fiber3 and fiber4[24]. The different spectral shape at the Ni L_2 edge (B1 and B2) also confirms the existence of NiO in fiber3 and fiber4[24]. The high oxidative state of Ni clusters may be from the oxidation of Ni in the air after the growth, while Fe clusters in CNTs is still dominated by the low chemical state. Both Fe and Ni are easy to be oxidized in air and the environmental geometry can be an important role for their chemical state. Here Fe exists in CNTs while Ni exists in CNFs. CNT shows a tube-like structure with concentric cylindrical carbon layers, Fe may migrate with the growth of CNTs and leave in the layers of CNTs. Fe on the inner carbon layers can be protected by the outside layer from oxidation and then shows a less oxidized chemical state. However, CNF shows a small hollow center and a thick wall without concentric cylindrical carbon layers. Thus Ni could contact more oxygen in air and be easily oxidized. The deference suggests the Ni clusters and Fe clusters in CNFs and CNTs, respectively, may also possess the different environment (e.g. the different interactions between Ni-CNF and Fe-CNT).

In conclusion, we have probed the electronic structure of CNTs and CNFs grown with Fe and Ni as catalyst, respectively, by STXM. The XANES results clearly show the catalyst-carbon interaction at the connection part of metal and carbon in the growth process. The catalyst clusters along the tube (fiber) were detected indicating a migration of the catalysts with the growth of CNTs (CNFs), which could help to explain the existence of atomic metal in CNT for the ORR. Different chemical states of the catalyst clusters are also observed in CNTs and CNFs. The STXM results reveal the

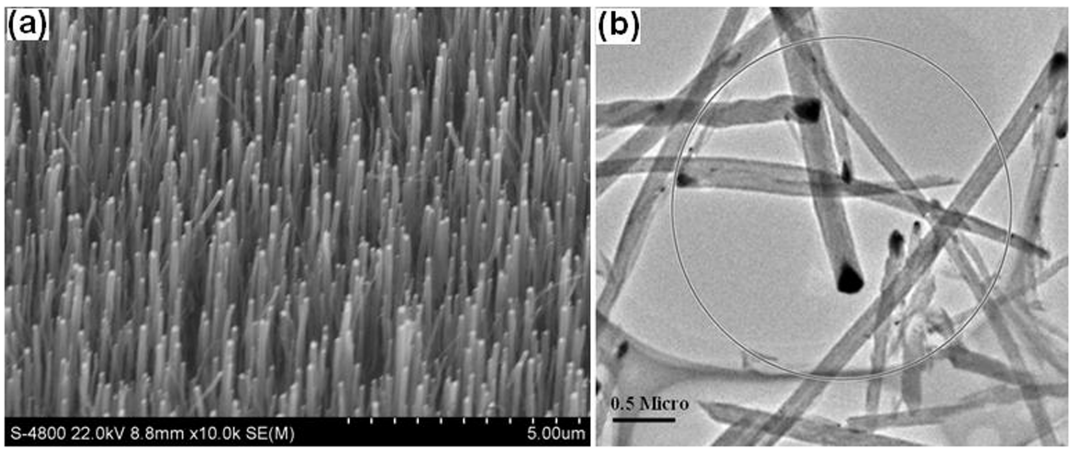

Figure 3 | (a) SEM and (b) TEM images of CNFs grown with 20 nm Ni/Ti underlayer.

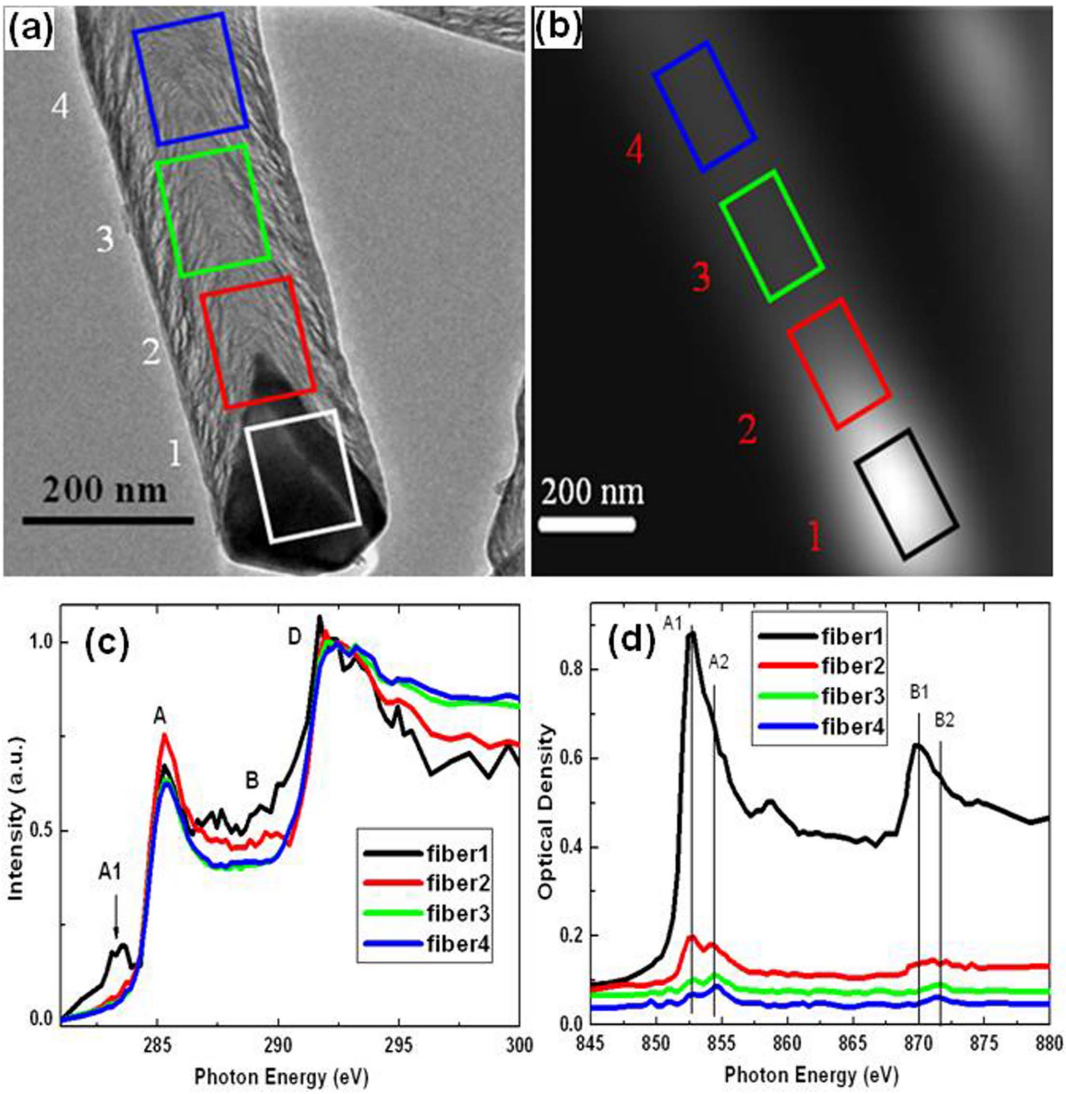

Figure 4 | (a) TEM image and (b) STXM map (at C *K*-edge) of CNFs, (c) Normalized C *K*-edge XANES spectra of fiber1–4 labeled in Fig. 4a and b, (d) Ni *L*-edge XANES spectra of fiber1–4 labeled in Fig. 4a and b.

distribution and chemical state of the growth catalysts in CNTs (CNFs), which may help to understand the role of catalysts when CNTs (CNFs) are used in various applications.

Methods

Synthesis of CNT and CNF. The growth of vertically aligned CNTs and CNFs by plasma-enhanced chemical vapor deposition (PECVD) was followed by a previous report in a Black Magic system (Aixtron Inc.)[16]. The metal underlayer (Ti) was evaporated directly on Si substrate to the thickness of 80 nm followed by the evaporation of Fe or Ni thin film (20 nm) as catalysts using electron-beam. Then the materials are pretreated by thermal annealing at 600°C under ~2 mbar NH_3 atmosphere for 3 min until the catalyst thin films were transferred into nanoparticles. Thereafter, a direct current PECVD was used to grow the carbon nanostructures which is an advantageous growth method achieving high yield and vertically aligned. In this proceeding, the substrate was first heated to desired growth temperature at 750°C and the mixed gas of NH_3 and C_2H_2 (4 : 1) were introduced into the reaction chamber to 7 Torr pressure. The plasma condition is 210 W with the applied voltage of 530 V. The growth period was 15 min for all samples. After growth, the samples were cooled down to room temperature before exposed to the air.

TEM and STXM measurement. All samples have been shown to be aligned carbon-based nanostructures on substrates[16]. CNTs (CNFs) were sonically dispersed in ethanol and then deposited on Cu grid for transmission electron microscopy (TEM) and STXM experiments. High-resolution transmission electron microscopy (FEI Tecnai G2 F20 S-TIWN) was used to characterize the morphology of samples. STXM experiments were performed on the SM beamline at the Canadian Light Source (CLS). STXM data were collected with a circularly polarized X-ray beam

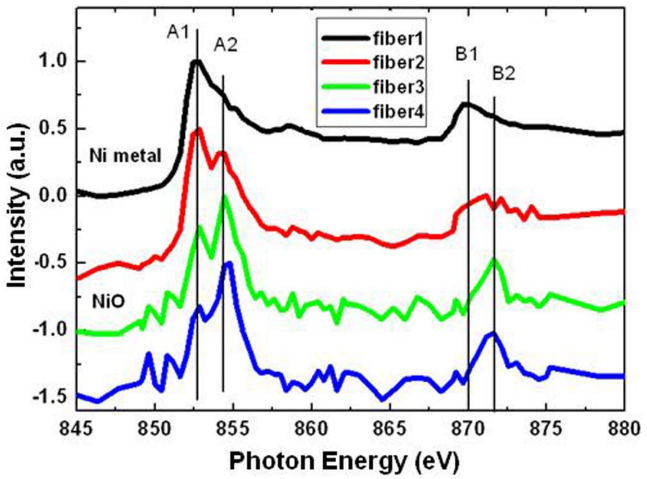

Figure 5 | Normalized Ni *L*-edge XANES spectra of fiber1–4 labeled in Fig. 4a and b.

perpendicular to the sample surface[10]. The focused X-ray beam is about 30 nm. The photon flux is about 2×10^7 photons/s. The image sequence (stack) scans over a range of photon energies have been used to obtain both chemically contrast imaging and XANES spectra[10,12]. STXM data were analyzed by *aXis2000* software.

1. Lefèvre, M., Proietti, E., Jaouen, F. & Dodelet, J. Iron-based catalysts with improved oxygen reduction activity in polymer electrolyte fuel cells. *Science* **324**, 71–74 (2009).
2. Lee, D. H., Lee, W. J., Kim, S. O. & Kim, Y. H. Theory, synthesis, and oxygen reduction catalysis of Fe-porphyrin-like carbon nanotube. *Phys. Rev. Lett.* **106**, 175502–175505 (2011).
3. Feng, X. L., Liu, R. L. & Wu, D. Nitrogen-doped ordered mesoporous graphitic arrays with high electrocatalytic activity for oxygen reduction. *Angew. Chem. Int. Edit.* **49**, 2565–2569 (2010).
4. Gong, K. P., Du, F., Xia, Z. H., Durstock, M. & Dai, L. M. Nitrogen-doped carbon nanotube arrays with high electrocatalytic activity for oxygen reduction. *Science* **323**, 760–764 (2009).
5. Liu, S. Q., Xu, X. A., Jiang, S. J. & Hu, Z. Nitrogen-doped carbon nanotubes: High electrocatalytic activity toward the oxidation of hydrogen peroxide and its application for biosensing. *ACS Nano* **4**, 4292–4298 (2010).
6. Li, Y. G. *et al.* An oxygen reduction electrocatalyst based on carbon nanotube-graphene complexes. *Nat. Nanotechnol.*, **7**, 394–400 (2012).
7. Burghard, M. Electronic and vibrational properties of chemically modified single-wall carbon nanotubes. *Surf. Sci. Rep.* **58**, 1–109 (2005).
8. Felten, A. *et al.* Measuring point defect density in individual carbon nanotubes using polarization-dependent x-ray microscopy. *ACS Nano* **4**, 4431–4436 (2010).
9. Schultz, B. J. *et al.* Imaging local electronic corrugations and doped regions in graphene. *Nat. Commum.* **2**, 372–379 (2011).
10. Zhou, J. G., Wang, J., Liu, H., Banis, M. N., Sun, X. L. & Sham, T. K. Imaging nitrogen in individual carbon nanotubes. *J. Phys. Chem. Lett.* **1**, 1709–1713 (2010).
11. Liang, Y. Y. *et al.* Co_3O_4 nanocrystals on graphene as a synergistic catalyst for oxygen reduction reaction. *Nat. Mater.* **10**, 780–786 (2011).
12. Felten, A. *et al.* Individual multiwall carbon nanotubes spectroscopy by scanning transmission X-ray microscopy. *Nano Lett.* **7**, 2435–2440 (2007).
13. Najafi, E. *et al.* Polarization. Dependence of the C 1s X-ray absorption spectra of individual multi-walled carbon nanotubes. *Small* **4**, 2279–2285 (2008).
14. Zhong, J. *et al.* Direct observation and spectroscopy of nanoscaled carboxylated carbonaceous fragments coated on carbon nanotubes. *Chem. Commun.* **47**, 8373–8375 (2011).
15. Li, J. *et al.* Carbon nanotube nanoelectrode array for ultrasensitive DNA detection. *Nano Lett.* **3**, 597–602 (2003).
16. Sun, X. H. *et al.* The effect of catalysts and underlayer metals on the properties of PECVD-grown carbon nanostructures. *Nanotechnology* **21**, 045201 (2010).
17. Kuznetsova, A. *et al.* Oxygen-containing functional groups on single-wall carbon nanotubes: NEXAFS and vibrational spectroscopic studies. *J. Am. Chem. Soc.* **123**, 10699–10704 (2001).
18. Liu, X., Pichler, T., Knupfer, M., Fink, J. & Kataura, H. Electronic properties of $FeCl_3$-intercalated single-wall carbon nanotubes. *Phys. Rev. B* **70**, 205405–9 (2004).
19. Hofmann, S. *et al.* In situ observations of catalyst dynamics during surface-bound carbon nanotube nucleation. *Nano Lett.* **7**, 602–608 (2007).
20. Emmenegger, C. *et al.* Synthesis of carbon nanotubes over Fe catalyst on aluminium and suggested growth mechanism. *Carbon* **41**, 539–547 (2003).
21. Yoshida, H., Takeda, S., Uchiyama, T., Kohno, H. & Homma, Y. Atomic-scale in-situ Observation of carbon nanotube growth from solid state iron carbide nanoparticles. *Nano Lett.* **8**, 2082–2086 (2008).
22. Smit de, E. *et al.* Nanoscale chemical imaging of a working catalyst by scanning transmission X-ray microscopy. *Nature* **456**, 222–225 (2008).
23. Arie, T., Nishijima, H., Akita, S. & Nakayama, Y. Carbon-nanotube probe equipped magnetic force microscope. *J. Vac. Sci. Technol. B* **18**, 104–106 (2000).
24. Regan, T. J. *et al.* Chemical effects at metal-oxide interfaces studied by X-ray-absorption spectroscopy. *Phys. Rev. B* **64**, 214422–124433 (2001).

Acknowledgments

We thank J. Wang, C. Karunakaran and Y. Lu for their support of experiments at CLS. Research at CLS is supported by NSERC, NRC, CIHR, and the University of Saskatchewan. We acknowledge the National Basic Research Development Program of China (2012CB825800, 2010CB934500), the National Natural Science Foundation of China (11179032, 11275137) and the Priority Academic Program Development of Jiangsu Higher Education Institutions (PAPD).

Author contributions

J.G. performed the sample preparation and characterization. J.G., L.B., J.L. and G.Z. carried out data analyses of STXM and contributed to writing the paper. J.Z. conducted the STXM examinations and analyses. J.Z. and X.S. proposed, planned and designed the project. J.Z. and X.S. supervised the project. All authors reviewed the manuscript.

Additional information

Competing financial interests: The authors declare no competing financial interests.

How to cite this article: Gao, J. *et al.* Revealing the Role of Catalysts in Carbon Nanotubes and Nanofibers by Scanning Transmission X-ray Microscopy. *Sci. Rep.* **4**, 3606; DOI:10.1038/srep03606 (2014).